

Contribution from the Department of Chemistry, University of California, Berkeley, California 94720, and Physics Department, Emory University, Atlanta, Georgia 30322

Coordination Chemistry of Microbial Iron Transport Compounds. 27. Dimeric Iron(III) Complexes of Dihydroxamate Analogues of Rhodotorulic Acid¹

SUSAN J. BARCLAY,² BOI HANH HUYNH,³ and KENNETH N. RAYMOND*²

Received December 9, 1983

A series of dihydroxamic acids $i\text{-C}_3\text{H}_7\text{N}(\text{OH})\text{C}(=\text{O})(\text{CH}_2)_n\text{C}(=\text{O})\text{N}(\text{OH})\text{-}i\text{-C}_3\text{H}_7$ ($n = 3\text{--}6, 8, 10$) are reported and the coordination properties of their iron(III) complexes described. The ligands model the microbial iron transport agent rhodotorulic acid and like that ligand form dimeric iron(III) complexes in aqueous and alcoholic solutions of composition Fe_2L_3 . Since the variation of ligand chain length changes the maximum Fe(III)–Fe(III) separation in the dimeric complexes, the complexes have been characterized by potentiometric titration, magnetic susceptibility, cyclic voltammetry, and electron paramagnetic resonance and Mössbauer spectroscopies. Solid-state, temperature-dependent magnetic susceptibility measurements for all of the Fe_2L_3 dimers give $\mu = 5.9 \pm 0.1 \mu_{\text{B}}/\text{Fe}^{3+}$, indicating there is no strong magnetic interaction between the paramagnetic iron centers. The cyclic voltammograms for $n = 6\text{--}10$ are characteristic of quasi-reversible one-electron reductions, indicating that the iron atoms in the dimeric complexes are reduced independently. For $n = 3$, the process appears similar to that for $n = 6\text{--}10$. For $n = 4$, $\Delta E = 41$ mV, suggesting a two-electron process. The cyclic voltammogram of the $n = 5$ complex reveals the presence of two reduction waves suggesting that there are at least two electroactive species in solution. The observed EPR resonance at $g = 4.3$ and the Mössbauer parameters ($\Delta E_{\text{Q}} = 0.63$ mm/s and $\delta = 0.6$ mm/s) confirm that the iron is high-spin ferric ion in a pseudooctahedral ligand field. The sextet ground state of the iron is split into three doublets that can be characterized by zero-field splitting parameters $D = 0.8$ cm⁻¹ and $E/D = 1/3$. Relaxation effects in the EPR and Mössbauer spectra of the iron complexes and Fe(III)-doped Al(III) complexes suggest a dipolar interaction between the ferric ions for shorter chains ($n = 3, 4, 6$), thus supporting a structure in which all three of the ligands occupy bridging positions. Comparison of the visible spectra of these complexes in methanol indicates that the complex with the $n = 5$ ligand, unlike the other complexes of this series, is no longer a tris(hydroxamato) complex but is instead a bis(hydroxamato) species that contains two methoxide ligands that bridge the two Fe^{3+} ions.

Introduction

The siderophores are low molecular weight chelating agents that are produced by microbes to solubilize and transport ferric ion to the cell.^{4,5} The hydroxamate group is one of the most common found in the siderophores produced by molds, fungi, and yeast. These compounds are predominantly trihydroxamic acids, which form very stable one-to-one complexes with ferric ion. In contrast, rhodotorulic acid (Figure 1) is a dihydroxamic acid, produced by *Rhodotorula pilimanae* and related yeasts,^{6–8} which is thus unable to satisfy the octahedral coordination about ferric ion through the formation of a one-to-one metal-to-ligand complex. It has been found to form dimeric complexes with Fe^{3+} , Al^{3+} , and Cr^{3+} with the formula $\text{M}_2(\text{RA})_3$.^{6,7} The structure proposed is one in which three ligands bridge the metal atoms, one isomer of which is shown in Figure 1.

Many monohydroxamate complexes have been prepared and studied as models for iron transport compounds in this laboratory^{9–11} and elsewhere.^{12,13} Although the preparation of several N-unsubstituted dihydroxamate ligands has been reported,^{14–16} they have not been used previously as siderophore

analogues but rather were prepared as analytical reagents. The succinyl, glutaryl, adipyl, and pimelyl bis(*N*-phenylhydroxamic acids) have been prepared by Ghosh and Sarkar;¹⁷ for $n = 2$ and 3 methylene groups separating the hydroxamic acid units (the succinyl and glutaryl derivatives, respectively), the ferric complexes were reported to be polymeric. For $n = 4$ and 5, the Al(III) complexes were proposed to be dimeric with only one bridging dihydroxamate ligand, the remaining two ligands forming large chelate rings in bis(bidentate) coordination to one metal ion.

We have prepared a series of ligands consisting of two *N*-isopropylhydroxamic acid groups separated by aliphatic chains of from 3 to 10 methylene groups. These compounds are both biological and physicochemical models of rhodotorulic acid. In this paper the physical properties of the ferric complexes are investigated to explore the plausibility of the various structures that have been proposed for the metal(III) complexes of rhodotorulic acid and its analogues. We conclude that the general structure shown in Figure 1 is correct for all the dimeric complexes studied. Molecular models show that by varying the chain length between the functional groups the distance between the metal ions of the dimeric complexes may be varied from approximately 5 to 12 Å. It was therefore of interest to determine what effect this variation of metal–metal distance would have on the chemical and physical properties of the metal complexes. We report here the preparation of the ferric dihydroxamate complexes, their characterization by IR, UV/vis, NMR, EPR, and Mössbauer spectroscopies, and their solution thermodynamic characterization by potentiometric titrations and cyclic voltammetry.

Experimental Section

Infrared spectra were obtained as KBr pellets on a Perkin-Elmer 597 spectrophotometer. Proton NMR spectra were recorded in $\text{CD}_3\text{OD}/\text{Me}_4\text{Si}$ solution on a Varian EM-390 spectrometer at 90 MHz. Melting points were taken in open capillaries by using a Mel-Temp apparatus and are uncorrected. Room-temperature magnetic susceptibility measurements were obtained by the NMR

- (1) Part 26: Barclay, S. J.; Riley, P. E.; Raymond, K. N. *Inorg. Chem.*, preceding paper in this issue.
- (2) University of California.
- (3) Emory University.
- (4) Raymond, K. N.; Tufano, T. P. "The Biological Chemistry of Iron"; Dunford, H. B., Dolphin, D., Raymond, K. N., Seiker, L., Eds.; D. Reidel Publishing Co.: Dordrecht, Holland, 1982; pp 85–105.
- (5) Neilands, J. B., Ed. "Microbial Iron Metabolism"; Academic Press: New York, 1974.
- (6) Mueller, G.; Barclay, S. J.; Raymond, K. N., submitted for publication.
- (7) Carrano, C. J.; Raymond, K. N. *J. Am. Chem. Soc.* **1978**, *100*, 5371.
- (8) Atkins, C. L.; Neilands, J. B. *Biochemistry* **1968**, *7*, 3734.
- (9) Abu-Dari, K.; Raymond, K. N. *J. Am. Chem. Soc.* **1977**, *99*, 2003.
- (10) Abu-Dari, K.; Barclay, S. J.; Riley, P. E.; Raymond, K. N. *Inorg. Chem.* **1983**, *22*, 3085.
- (11) Raymond, K. N.; Abu-Dari, K.; Sofen, S. R. "Stereochemistry of Optically Active Transition Metal Compounds"; Douglas, B. E., Saito, Y., Eds.; American Chemical Society: Washington, DC, 1980; ACS Symp. Ser. No. 119, pp 133–167.
- (12) Brown, D. A.; Chidambaram, M. V.; Glennon, J. D. *Inorg. Chem.* **1980**, *19*, 3260.
- (13) Monzyk, B.; Crumbliss, A. L. *J. Am. Chem. Soc.* **1979**, *101*, 6203.
- (14) Hurd, C. D.; Botteran, D. G. *J. Org. Chem.* **1946**, *11*, 207.
- (15) Hines, J. W., Jr.; Stamm, C. H. *J. Med. Chem.* **1977**, *20*, 965.

- (16) Fishman-Goldenberg, V.; Spoerri, P. E. *Anal. Chem.* **1959**, *31*, 1735.
- (17) Ghosh, N.; Sarkar, D. *J. Indian Chem. Soc.* **1968**, *45*, 550; **1969**, *46*, 528; **1970**, *47*, 562, 723; **1973**, *50*, 415.

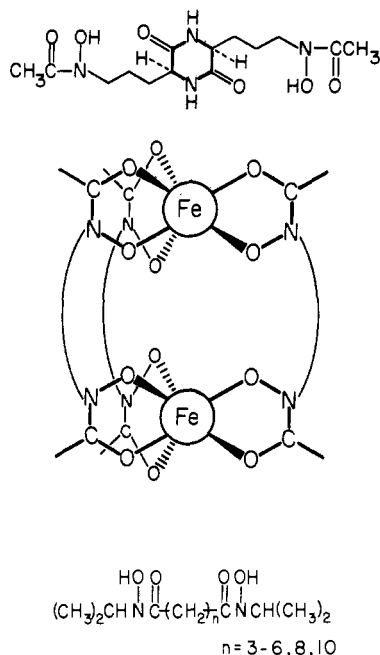


Figure 1. Structural formula of rhodotorulic acid, the synthetic dihydroxamate ligands reported here, and the proposed structure for the dimeric ferric dihydroxamate complexes.

method¹⁸ in methanol solution. Microanalyses were performed by Analytical Services, Chemistry Department, University of California, Berkeley.

Preparation of Compounds. Syntheses of the adipyl, suberyl, sebacyl, and dodecanediyl bis(*N*-isopropyl hydroxamic acids) have been reported.¹⁹ Similar conditions were used to prepare the glutaryl and pimelyl analogues.

N,N'-Dihydroxy-*N,N'*-diisopropylpentanediamide: IR (cm⁻¹) ν 3.165 (s, OH), 1600 (s, C=O); NMR (CD₃OD) δ 1.18 (d, 12 H, (CH₃)₂C<), 1.90 (quintet, 2 H), 2.50 (t, 4 H, -CH₂C(O)-), 4.65 (septet, 2 H, HC<); mp 126–128 °C; yield 35%. Anal. Calcd for C₁₁H₂₂N₂O₄: C, 53.66; H, 8.94; N, 11.38. Found: C, 53.78; H, 9.00; N, 11.32.

N,N'-Dihydroxy-*N,N'*-diisopropylheptanediamide: IR (cm⁻¹) ν 3165 (s, OH), 1600 (s, C=O); NMR (CD₃OD) δ 1.15 (d, 12 H, (CH₃)₂C<), 1.37 (quintet, 2 H), 1.62 (quintet, 4 H), 2.45 (t, 4 H, -CH₂C(O)-), 4.65 (septet, 2 H, HC<); mp 128–130 °C; yield 60%. Anal. Calcd for C₁₃H₂₆N₂O₄: C, 56.93; H, 9.49; N, 10.22. Found: C, 56.96; H, 9.55; N, 10.13.

The ferric complexes were prepared by reacting a slight excess of ferric acetylacetonate with free ligand. A typical synthesis is as follows:

Solid Fe(acac)₃ (0.30 g, 0.85 mmol) was added with stirring to a methanolic solution (50 mL) of 0.41 g (1.19 mmol) of *N,N'*-dihydroxy-*N,N'*-diisopropyldecanediamide. The mixture was left at room temperature for 1 day, after which the methanol and acetylacetonate were removed in vacuo. After first washing with diethyl ether to remove any unreacted Fe(acac)₃, the solid was redissolved, with heating, in a minimum volume of 1:1 MeOH/CCl₄. Precipitation of the complex from this solution by the addition of petroleum ether and drying in vacuo (60 °C, 1 day) gave 0.32 g (0.28 mmol, 71% yield) of an orange hygroscopic powder.

Ferric complexes of the other dihydroxamic acids were prepared by using the same procedure:

Diferric tris(*N,N'*-dihydroxy-*N,N'*-diisopropyldecanediamide): IR (cm⁻¹) ν (C=O) 1555, 1562; μ = 5.7 μ_B . Anal. Calcd for Fe₂(C₁₈H₃₄N₂O₄)₃·H₂O: C, 56.00; H, 8.99; N, 7.27. Found: C, 55.81; H, 8.88; N, 7.07.

Diferric tris(*N,N'*-dihydroxy-*N,N'*-diisopropyldecanediamide): IR (cm⁻¹) ν (C=O) 1556, 1562; μ = 5.8 μ_B . Anal. Calcd for Fe₂(C₁₆H₃₀N₂O₄)₃·H₂O: C, 53.73; H, 8.58; N, 7.84. Found: C, 53.87; H, 8.32; N, 7.58.

Diferric tris(*N,N'*-dihydroxy-*N,N'*-diisopropyloctanediamide): IR (cm⁻¹) ν (C=O) 1555, 1562; μ = 5.8 μ_B . Anal. Calcd for Fe₂(C₁₄H₂₆N₂O₄)₃·H₂O: C, 51.03; H, 8.10; N, 8.50. Found: C, 51.17; H, 8.07; N, 8.33.

Diferric tris(*N,N'*-dihydroxy-*N,N'*-diisopropylheptanediamide): IR (cm⁻¹) ν (C=O) 1555, 1560; μ = 4.8 μ_B . Anal. Calcd for Fe₂(C₁₃H₂₄N₂O₄)₃·H₂O: C, 49.47; H, 7.82; N, 8.88. Found: C, 49.86; H, 7.62; N, 8.66.

Diferric tris(*N,N'*-dihydroxy-*N,N'*-diisopropylhexanediamide): IR (cm⁻¹) ν (C=O) 1556, 1562; μ = 5.9 μ_B . Anal. Calcd for Fe₂(C₁₂H₂₂N₂O₄)₃·H₂O: C, 47.79; H, 7.52; N, 9.28. Found: C, 48.00; H, 7.43; N, 8.93.

Diferric tris(*N,N'*-dihydroxy-*N,N'*-diisopropylpentanediamide): IR (cm⁻¹) ν (C=O) 1554, 1560; μ = 5.8 μ_B . Anal. Calcd for Fe₂(C₁₁H₂₀N₂O₄)₃·H₂O: C, 45.94; H, 7.19; N, 9.74. Found: C, 45.80; H, 6.87; N, 9.35.

Molecular Weight Determinations. Measurements for the tris-(hydroxamate) complexes were made on a Sephadex LH-20 column. The eluting solvent was 0.023 M NaOAc in MeOH, and a flow rate of 2 mL/min was used. The column was standardized by using ferric rhodotorulate, ferric benzohydroxamate, and ferric *N*-phenylbenzohydroxamate. Measurements for the bis complexes were made on a Biogel P-2 column using aqueous HCl (pH 2) as the eluting solvent with a flow rate of 0.5 mL/min. The column was calibrated with [Co(EDTA)]⁻ and vitamin B₁₂.

Spectrophotometric Titrations. Visible spectra were recorded by using Hewlett-Packard 8450A or Cary 118 UV/vis spectrophotometers. The spectra were measured as a function of pH in methanol solution for $n = 3$ –10 and in water for $n = 3$ –6. Adjustments of pH were made by addition of nitric acid.

Spectrophotometric competition experiments were performed with 10-mL aqueous samples in which free EDTA was added to a solution of ferric hydroxamate complex or, alternatively, free dihydroxamate ligand was added to a solution of ferric EDTA. The solutions were 0.1 M ionic strength (KNO₃). The pH measurements were made with use of a Brinkmann Instruments Model pH-102 digital meter equipped with a glass calomel combination electrode (Sigma). The pH was adjusted with KOH or HNO₃ to obtain a value at equilibrium of between 6 and 7. The solutions were allowed to equilibrate from 2 to 3 weeks, until a constant pH was obtained.

Potentiometric Titrations. Samples (40 mL) were placed in a jacketed titration cell maintained at 25 °C by a circulating constant-temperature bath. All titrations were carried out under positive argon pressure and 0.1 M ionic strength (KNO₃). The pH measurements were made with a Corning Model 130 digital pH meter equipped with Corning glass and saturated calomel electrodes. The meter was standardized (with nitric and acetic acid) to read hydrogen ion concentration instead of activity. Refinement of the potentiometric data was performed by a nonlinear least-squares program.²⁰

Electron Spin Resonance. EPR spectra were obtained in frozen methanol solutions at -140 and -260 °C, on Varian E-3 and E-9 spectrophotometers with liquid-nitrogen- and liquid-helium-flowing cryostats, respectively. The complexes were generated in situ by addition of ferric nitrate to a slight excess of ligand. The solutions were 1 mM in Fe³⁺, and the pH was adjusted to between 7 and 8. The mixed iron–aluminum complexes were also formed in situ by addition of ferric nitrate to a solution of the aluminum complex such that the solutions were 0.1 mM Fe³⁺ and 10 mM Al³⁺.

Mössbauer Spectra. The Mössbauer spectrometer at Emory University is of the constant-acceleration type and has been described elsewhere.²¹ Room-temperature spectra of a metallic iron foil are used to calibrate the velocity scale, and the centroid of these spectra is taken as zero velocity.

Magnetic Susceptibility Measurements. Low-temperature magnetic susceptibility measurements were performed by using powdered samples in holders machined from Kel-F. Measurements for $n = 4$,

- (20) The least-squares program varied the set of equilibrium constants to minimize the function $R = \sum w(pH_{\text{obsd}} - pH_{\text{calcd}})^2$. The weighting factor w is defined by $1/w = [\sigma(pH)]^2 = \sigma_e^2 + \sigma_v^2(\partial pH/\partial V)^2$ where the standard deviation of any given pH measurement, $\sigma(pH)$, is determined by the intrinsic error in pH measurement, σ_e , plus the error resulting from an error in the volume of titrant delivered (0.002 mL), which is propagated by the slope of the titration curve at pH_{obsd} , $\partial pH/\partial V$. This weighting scheme minimizes the importance of the less reliable data from regions of steep slope relative to the data from the buffer regions.
- (21) Huynh, B. H.; Lui, M. C.; Moura, J. J. G.; Moura, I.; Ljungdahl, P. O.; Munck, E.; Payne, W. J.; Peck, H. D., Jr.; Der Vartanian, D. V.; LeGall, J. *J. Biol. Chem.* **1982**, *257*, 9576.

(18) Evans, D. F. *J. Chem. Soc.* **1959**, 2003.

(19) Smith, W. L.; Raymond, K. N. *J. Am. Chem. Soc.* **1980**, *102*, 1252.

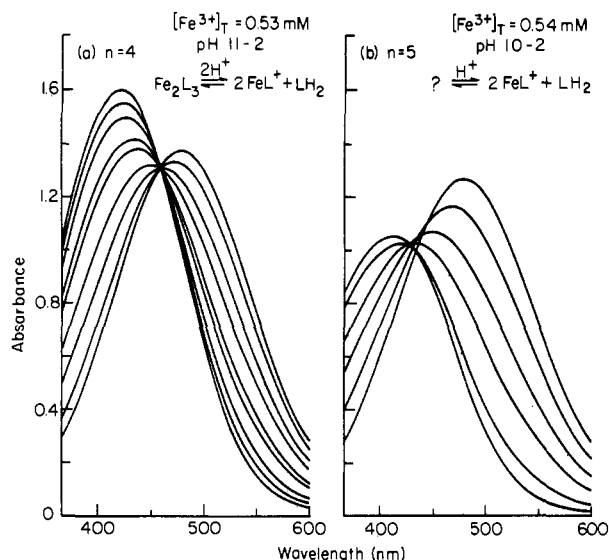


Figure 2. Spectrophotometric titrations of ferric dihydroxamate complexes in methanol ($\text{Fe}:\text{L} = 2:3$): (a) $n = 4$; (b) $n = 5$.

6, 8, and 10 were made on a PAR Model 1555 vibrating-sample magnetometer used with a homogeneous magnetic field produced by a Varian Associates 12-in. electromagnet capable of a maximum field strength of 12.5 kG; the results were averaged in calculating the effective magnetic moment. A liquid-helium Dewar produced sample temperatures in the range 3.8–80 K, which were measured with a calibrated GaAs diode approximately 1 cm above the sample (~ 40 mg). The magnetometer was calibrated with $\text{HgCo}(\text{NCS})_4$, and the resulting susceptibilities were corrected for underlying diamagnetism. Measurements for complexes with $n = 3$ and 5 were made with a SHE Model 805 variable-temperature susceptometer capable of a maximum field strength of 50 kG in conjunction with a SHE Model 868 susceptometer control system.

Electrochemistry. Electrochemical measurements were made by using a three-electrode configuration with hanging-mercury-drop working electrode, platinum-wire auxiliary electrode, and saturated calomel reference electrode. The scan rate was 100 mV/s. All potentials are reported vs. SCE and are uncorrected for liquid-junction potentials. Triangular waves were generated by the Princeton Applied Research (PAR) 175 programmer in conjunction with the PAR 173 potentiostat. Solvent systems used were methanol/water mixtures with 0.1 M tetraethylammonium tetrafluoroborate or perchlorate as supporting electrolyte. Ferric complexes were generated in situ by addition of methanolic FeCl_3 to a solution of ligand. The pH was adjusted with triethylamine.

Results and Discussion

Solution Equilibria. Examination of the pH dependence of the ferric dihydroxamate visible spectra in methanol reflects the presence of three sequential complexation reactions. For all of the ligands except $n = 5$, the complex at high pH gives an orange-red solution with λ_{max} 424 nm (ϵ 3000–3400/Fe). As the pH is lowered from 11.0 to 1.0, isosbestic behavior is observed with isosbestic points at 461–468 nm, and a red bis(hydroxamato) complex is formed with λ_{max} 480 nm (ϵ 2500–3000/Fe). As the pH is lowered further (pH < 0), another isosbestic point is observed as the purple (λ_{max} 520 nm) monohydroxamate complex is formed. Figure 2a shows the visible spectrum as a function of pH for $n = 4$.

The behavior of the $n = 5$ complex in methanol (Figure 2b) is strikingly different from the others at high pH. As the pH of a solution of the red bis(hydroxamato) complex is raised, the peak at 480 nm (ϵ 2600) shifts with a decrease in intensity to a final value of 413 nm (ϵ 2100) at pH 7 (further raising to pH 10 results in no change in the spectrum). The final color of the solution is yellow, rather than the orange-red that is characteristic of ferric tris(hydroxamato) complexes (λ_{max} ~ 425 nm). As a general rule, the extinction coefficient of a ferric hydroxamate is approximately $1000n \text{ M}^{-1} \text{ cm}^{-1}$, where

n is the number of hydroxamate moieties bound per ferric ion. The decrease in extinction coefficient with increasing pH for the ferric $n = 5$ complex suggests displacement of a hydroxamate ligand, possibly due to the formation of a ferric methoxy species. The absence of an isosbestic point in Figure 2b suggests the presence of at least three species in solution; presumably the FeL^+ cation, the Fe_2L_3 dimer, and an anomalous $n = 5$ iron complex. The isolation and structural characterization of this anomalous $n = 5$ complex as the bis(μ -methoxy)-bridged species $\text{Fe}_2\text{L}_2(\mu\text{-OCH}_3)_2$ has been described in detail.^{1,22} However, at low pH the $n = 5$ complex exhibits the spectral characteristic of the usual bis- to mono-(hydroxamato) equilibrium.

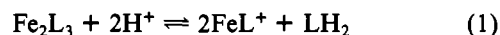
As the pH of aqueous solutions of the ferric tris(hydroxamato) complexes with $n = 3$ –6 is lowered ($n = 8$ and 10 are not sufficiently water soluble), the visible spectrum exhibits changes similar to those observed in methanol. Even the behavior of the $n = 5$ ligand is identical with that of the others in aqueous solution. However isosbestic behavior is observed over a smaller range of pH values than in methanol, due to formation of hydroxy species above pH 9.

The iron-binding properties of the dihydroxamate ligands were examined at low pH by using the mole ratio method. Aliquots of a standardized acidic ferric nitrate solution were added to a methanolic solution of the ligand, and the absorbance was measured at λ_{max} for each mole ratio. The mole ratio plots at prevailing pH (≈ 2) establishes the stoichiometry of the complexes to be $(\text{FeL}^{n+})_x$. Potentiometric titration curves for 2:3 $\text{Fe}:\text{LH}_2$ solutions show a single break at 3 equiv of base per iron, verifying the formation of tris(hydroxamato) complexes $(\text{Fe}_2\text{L}_3)_x$.

Approximate molecular weight measurements were made by using gel partition chromatography. This was done in order to demonstrate (1) that the nature of the tris(hydroxamato) complexes is dimeric ($x = 1$) rather than polymeric ($x = \infty$) and (2) that the bis(hydroxamato) complexes are monomeric, as has been demonstrated for rhodotorulic acid.⁷

All of the tris(dihydroxamato) complexes were found to have approximately the same elution volume, corresponding to an average molecular weight of 1320 (actual values for dimeric complexes are 900–1140). Molecular weight measurements for the bis complexes gave values of 309–394 (actual values for monomeric species are 300–398, and for the dimeric species 600–796).

These results show that the equilibrium giving rise to the isosbestic point at 465 nm is



Attempts to obtain crystalline samples of the Fe_2L_3 complexes for X-ray structural analysis were unsuccessful. The powders that were obtained were amorphous, as evidenced by the fact that they do not diffract X-rays. Although the complexes are extremely soluble in methanol, the redissolution of the solid compounds is very slow and requires heating. The chemically inert chromic complexes on the other hand dissolve readily in alcohol solutions. These observations suggest that although the tris(hydroxamato)iron(III) complexes are dimeric in solution, they may be polymeric in the solid state.

Potentiometric Titrations. Titration curves for the free ligands with $n = 3$ –6 are shown in Figure 3. The data for $n = 4$ –6 were fit on the assumption that the two hydroxamate protons have similar but slightly different pK_a 's. The titration curve for the glutaryl derivative differs from the others in that the pK_a 's of the two protons are sufficiently different to give rise to two separate buffer regions corresponding to their removal. The calculated proton dissociation constants for the

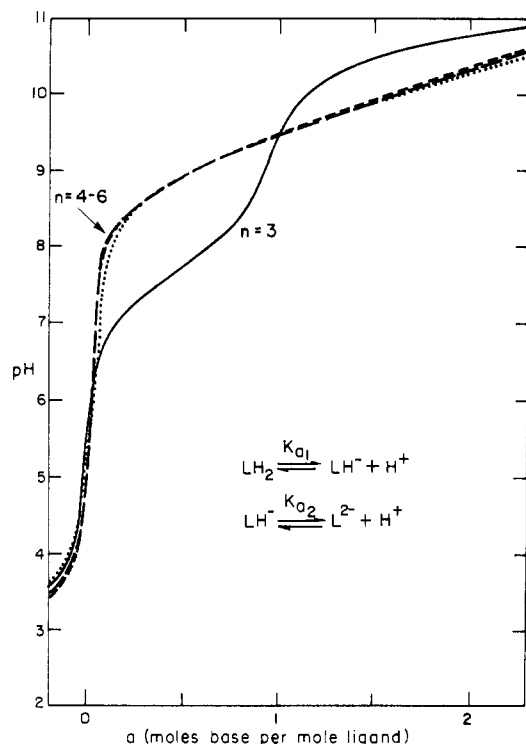


Figure 3. Potentiometric titration curves for dihydroxamate ligands with $n = 3-6$ in aqueous solution.

Table I. Proton Dissociation Constants for Dihydroxamic Acids^a

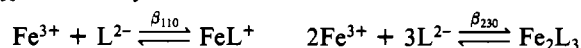
n	pK_1	pK_2	n	pK_1	pK_2
3	7.74 (4)	10.79 (2)	6	9.21 (3)	9.78 (3)
4	9.10 (2)	9.79 (3)	RA	8.49 (3)	9.44 (3)
5	9.16 (2)	9.83 (2)			

^a Measured in 0.1 M KNO_3 , 25 °C.

free ligands are given in Table I, with those for RA²³ listed for comparison.

The proton dissociation constants obtained for the dihydroxamate ligands are within the range ($pK_a = 8-10$) expected for hydroxamic acids.²⁴ The $n = 3$ ligand is strikingly different, with the two pK_a values differing by 3 orders of magnitude. This behavior we ascribe to intramolecular hydrogen bonding in the monoprotonated $n = 3$ ligand. For a molecule with two identical and noninteracting acid sites, statistics lead to a difference in the two acid constants such that $pK_{a2} - pK_{a1} = 0.602$.²⁵ The quantity $pK_{a2} - pK_{a1}$ decreases from 3.05 (4) for $n = 3$ to 0.57 (4) for $n = 6$. This indicates that for $n = 6$ the acid sites are essentially noninteracting, whereas for $n = 3$ there is a relatively large inductive effect. There is a monotonic change in this interaction for the intermediate values $n = 4$ and 5.

Titration curves for the ferric complexes ($\text{Fe:LH}_2 = 2:3$) are shown in Figure 4. The equivalence point occurs at 3 equiv of H^+ per iron. From the ligand protonation constants and the potentiometric data from the iron-ligand titrations, refinement was attempted of the stability constants β_{110} and β_{230} , defined by



(23) Carrano, C. J.; Cooper, S. R.; Raymond, K. N. *J. Am. Chem. Soc.* **1979**, *101*, 599.

(24) Martell, A. E.; Smith, R. M. "Critical Stability Constants"; Plenum Press: New York, 1974; Vol. I, p 207.

(25) For two equivalent, noninteracting protons (with an intrinsic, monomeric acid dissociation constant K) at acid sites that are identical but distinguishable, the observed acid dissociation constants are $K_{a1} = 2K$ and $K_{a2} = K/2$ such that $pK_{a2} - pK_{a1} = \log 4 = 0.602$. See: Adams, E. Q. *J. Am. Chem. Soc.* **1916**, *38*, 1503.

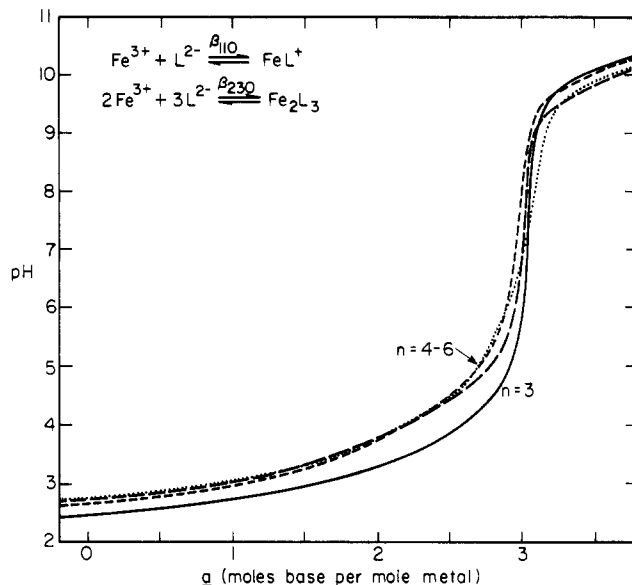


Figure 4. Potentiometric titration curves for ferric dihydroxamate complexes ($\text{Fe:LH}_2 = 2:3$; $n = 3-6$).

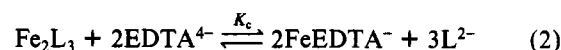
Table II. Formation Constants for Ferric Dihydroxamate Systems^a

n	$\log \beta_{230}$	$\log \beta_{110}$	pM^b
3	62.1 (3)	22.84 (5)	20.69
4	62.2 (3)	22.83 (5)	20.39
5	62.4 (2)	22.76 (6)	20.24
6	62.3 (2)	22.63 (4)	20.23
RA	62.2 (1)	21.55 (8)	21.76

^a Measured in 0.1 M KNO_3 , 25 °C. ^b $pM = -\log [\text{Fe}^{3+}]$ for pH 7.4 solutions containing 10^{-8} M total iron and 10^{-6} M total ligand.

using as initial guesses the values determined for RA.²³ Correlation between these constants was too great to refine both values simultaneously. It was necessary to obtain an independent value for one in order to solve for the other; thus, β_{230} was determined through EDTA competition experiments.

Competition Experiments. Between pH 6 and 7 and in the presence of excess dihydroxamate ligands, the only complex present in significant concentration is the dimer Fe_2L_3 . Thus competition between LH_2 and EDTA, when written in terms of the fully deprotonated ligand concentrations, is described by



$$K_c = [\text{L}]^3 [\text{FeEDTA}]^2 / [\text{Fe}_2\text{L}_3] [\text{EDTA}]^2 \quad (3)$$

This may be written as

$$\beta_{230} = \frac{[\text{Fe}_2\text{L}_3]}{[\text{Fe}]^2 [\text{L}]^3} = \frac{(\beta_{110}^{\text{EDTA}})^2}{K_c} \quad (4)$$

where

$$\beta_{110}^{\text{EDTA}} = \frac{[\text{FeEDTA}]}{[\text{Fe}][\text{EDTA}]} = 10^{25} \quad (5)^{26}$$

In order to demonstrate that mixed hydroxamate-EDTA complexes are not formed during the competition experiments, the visible spectrum was measured as a function of time for solutions containing Fe_2L_3 to which an excess of EDTA was added. The presence of an isosbestic point throughout the reaction demonstrates that there are only two absorbing species

(26) Martell, A. E.; Smith, R. M. "Critical Stability Constants"; Plenum Press: New York, 1974; Vol. III, pp 301-305.

in solution: Fe_2L_3 and $[\text{FeEDTA}]^-$.

From the known protonation constants for the dihydroxamic acids and EDTA, and equilibrium pH and absorbance measurements, with the appropriate mass-balance equations, the formation constants for the tris complexes, β_{230} , were calculated. The values obtained (Table II) are within experimental error to that determined for rhodotorulic acid ($\log \beta_{230}^{\text{RA}} = 62.2$).²³ With $\log \beta_{230}$ used as a fixed parameter in the refinement of the potentiometric titration data, the values for β_{110} (Table II) were obtained.

The formation constants for the tris(hydroxamato) complexes were found to be identical within experimental error over the entire range of chain lengths from $n = 3$ to $n = 6$ to that obtained for RA. Thus, even as the hydroxamate groups are brought closer together within the same molecule, no "macrochelate effect" is observed. The calculated values of β_{110} are 1–2 orders of magnitude greater than values reported for other mono-, di-, and trihydroxamic acids, but this difference is not substantial in terms of a chelate effect. This confirms the observation that the formation constants for ferric hydroxamate complexes depend only on the number of hydroxamate groups bound to iron and not on whether they are part of a multichelate molecule or independent ligands.²³

The relative abilities of weak acid ligands to bind ferric ion are best determined by calculating the equilibrium concentration of hexaaquoiron(III) present in a solution of specified pH and total iron and total ligand concentrations. The pM ($-\log [\text{Fe}^{3+}]$) values (Table II) indicate that RA is a slightly better ligand than the synthetic models for the binding of ferric ion, as expected due to the lower $\text{p}K_a$ values of the RA ligand.

Magnetic Measurements. Temperature-dependent magnetic susceptibility measurements on the complexes $\text{Fe}_2\text{L}_3 \cdot \text{H}_2\text{O}$ for chain lengths $n = 3$ –6, 8, and 10 indicate that the iron is high-spin ferric ion over the entire range of chain lengths. The complexes exhibit Curie–Weiss behavior; the magnetic moments calculated from the slopes of the $1/\chi_m'$ vs. T plots (obtained by fitting the data with a linear least-squares program) are $5.9 \pm 0.1 \mu_B$ over the entire range of chain lengths as expected for high-spin ferric ion ($\mu_{\text{spin only}} = 5.92 \mu_B$). This indicates the absence of any strong magnetic interactions (i.e., no coupling of electron spins) between the iron sites in the complexes. These results are in agreement with the solution magnetic susceptibility measurements. The exception is the $n = 5$ complex, which exhibits a reduced moment ($\mu_{\text{eff}} \sim 4.8 \mu_B$) in methanol solution at room temperature.

Electron Paramagnetic Resonance. The EPR spectra of the ferric dihydroxamate complexes were measured in frozen methanol solutions, with a total iron concentration of 1 mM. At this concentration, intermolecular spin–spin interactions are negligible.²⁷ The spectra of 0.1 mM solutions were identical with those of 1 mM solutions. All of the complexes were found to be EPR active with a resonance observed at $g = 4.3$, characteristic of high-spin, octahedral ferric ion. Castner et al.²⁸ have shown that a spin Hamiltonian

$$\hat{H}_f = D[S_z^2 - S(S+1)/3 + (E/D)(S_x^2 - S_y^2)] \quad (6)$$

with $E/D = 1/3$ will split the 6S state of ions such as high-spin Fe^{3+} into three doublets, the middle one having an isotropic g value of 4.286. A peak at $g \sim 4.3$ has also been observed at temperatures between 300 and 1 K in the EPR spectrum of the naturally occurring tris(hydroxamato) siderophore complex ferrichrome A.²⁹ Temperatures of 1 K were nec-

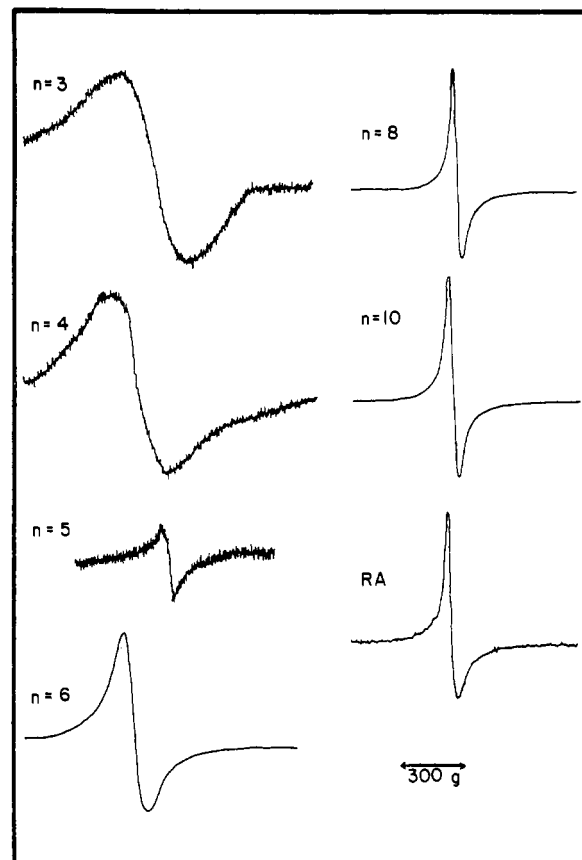


Figure 5. EPR spectra of ferric dihydroxamate complexes in frozen methanol ($\text{Fe:L} = 2:3$; $\text{pH}^* = 7$ –8; $[\text{Fe}^{3+}] = 1$ mM (except for the RA complex, where $[\text{Fe}^{3+}] = 0.1$ mM); microwave power 10 mW; $T = -140$ °C; $\nu = 9.115$ GHz; modulation frequency 10 kHz).

Table III. g Values and Line Widths for Ferric Dihydroxamate Complexes in MeOH at -140 °C

n	g	$\Delta H(\text{Fe}_2\text{L}_3)$, G	$\Delta H(\text{FeAIL}_3)$, G
3	4.28	335	47
4	4.30	230	45
5	4.31	70 (w)	53
6	4.33	120	46
8	4.36	45	43
10	4.34	52	49
RA	4.37	51	46
BHA ^a	4.34	43	

^a BHA = benzohydroxamic acid.

essary in order to observe additional resonances at g values of 9.6, 1.3, and 1.0, attributable to transitions arising from the lower Kramers doublet. The EPR spectra of the ferric dihydroxamate complexes at 13 K reveal an additional weak resonance at $g \sim 9$ –10; temperatures lower than this were not investigated.

The EPR spectra of the ferric dihydroxamate complexes at -140 °C ($\text{Fe:L} = 2:3$) are shown in Figure 5 and the results summarized in Table III. The line widths of the $g = 4.3$ signals were unchanged at -260 °C. The spectra of the complexes with chain lengths $n = 8$ and 10 are essentially identical with those for ferric rhodotorulate and the monomeric complex ferric benzohydroxamate. This indicates that the metal atoms in the dimeric complexes are equivalent and are sufficiently well separated that they are noninteracting. As the chain length is decreased from 8, the shape of the $g = 4.3$ signal changes significantly. The line width increases with decreasing chain length from 120 G for $n = 6$ to 335 G for $n = 3$. The broadening of the signals is accompanied by a decrease in intensity (as expected for dipolar broadening, since

(27) Wickman, H. H.; Klein, M. P.; Shirley, D. A. *Phys. Rev.* **1966**, *152*, 345.

(28) Castner, T.; Newell, G. S.; Holton, W. C.; Slichter, C. P. *J. Chem. Phys.* **1960**, *32*, 668.

(29) Wickman, H. H.; Klein, M. P.; Shirley, D. A. *J. Chem. Phys.* **1965**, *42*, 2113.

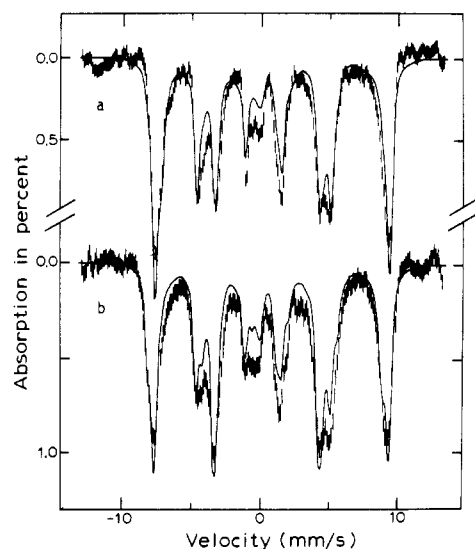


Figure 6. Mössbauer spectra of the $n = 10$ ferric dihydroxamate complex in frozen methanol. The data are recorded at 4.2 K (a) and 10 K (b) with a 500-G field applied parallel to the γ beam. The solid lines are theoretical spectra simulated with spin Hamiltonian parameters listed in the text.

the area under the absorption curve must remain constant for equal concentrations of identical paramagnetic species).

One possible cause for this broadening effect is a dipole-dipole interaction between the ferric ions in the dimeric complexes. Molecular models indicate that the maximum distance between the metal centers in the $n = 6$ complex (the structure shown in Figure 1) is approximately 8.5 Å. Dipolar broadening might be expected at this distance for a spin $5/2$ system. Theoretical calculations by Aasa et al.³⁰ suggest that magnetic dipole-dipole interactions are significant for high-spin ferric ion at distances less than 9 Å. Such an effect is analogous to the broadening of EPR signals of concentrated solutions of paramagnetic species. In this case, however, it is due to an increase in the "effective" Fe^{3+} concentration caused by restricting the two iron centers to remain in close proximity to one another. That is, the interaction is essentially *intramolecular* rather than *intermolecular*.

Another possible cause for the broadening of the EPR spectra for this series of complexes could be a small, systematic change in the coordination environment of the ferric ions as the chain length decreases (possibly due to steric strain). If this change causes the crystal field parameter E/D to vary significantly from $1/3$, the g value for the middle Kramers doublet will no longer be isotropic, thus causing a broadening of the EPR signal. To eliminate this as a possible explanation, EPR spectra of mixed Fe-Al dihydroxamate complexes were obtained and the linewidths of the $g = 4.3$ signal are listed in Table III. The line widths are approximately 50 G over the entire range of chain lengths and are identical with those observed for the diferric complexes with the longer chain lengths of 8 and 10. This provides further evidence that the line broadening observed in the EPR spectra of the diferric complexes with the shorter chains is due to a dipolar interaction between the metal centers, thus supporting the structure shown in Figure 1 for these complexes.

The EPR resonance for the $n = 5$ complex is very weak relative to those of the other dihydroxamate complexes. This is consistent with a relatively strong interaction between the two iron sites, as has been confirmed for this methoxide-bridged dimer.^{1,22}

Mössbauer Experiments. The Mössbauer spectra of ^{57}Fe dihydroxamate complexes with $n = 3, 5,$ and 10 have been studied in frozen methanol. Mössbauer spectra of the $n = 10$ complex are shown in Figure 6. The spectra were measured at 4.2 K (Figure 6a) and 10 K (Figure 6b) with a magnetic field of 500 G applied parallel to the γ beam. The observation of a well-resolved hyperfine pattern demonstrates that the electronic relaxation rate is slow compared to the nuclear precession frequency (10^7 s^{-1}).

The spectra shown in Figure 6 are superpositions of spectral components arising from the ground and middle Kramers doublets and indicate the presence of a single high-spin ferric species. The ground doublet yields a six-line absorption spectrum that extends from -8 to $+9$ mm/s. The line intensity ratios are approximately 3:2:1:1:2:3. The intensity pattern implies an easy axis of magnetization for the ground doublet,³¹ i.e., the electronic g tensor is extremely anisotropic. The middle doublet exhibits a four-line spectrum with the outermost lines appearing in the -3 and $+4$ mm/s regions. The line intensities depend strongly on the direction of the applied field, suggesting a fairly isotropic g tensor for the middle doublet. These observations and the $g = 4.3$ EPR signal indicate that the electronic ground state of the iron may be described by the fine structure term of eq 6 where $S = 5/2$ and $E/D = 1/3$. Such an electronic state has an extremely anisotropic g tensor ($g_x = 0.8, g_y = 0.6, g_z = 9.7$) for the ground doublet and an isotropic one ($g_x = g_y = g_z = 4.3$) for the middle doublet.

To analyze the Mössbauer spectra, we use the spin Hamiltonian of eq 6 and the Zeeman, magnetic and electric hyperfine interaction, and nuclear Zeeman terms

$$\hat{H} = g\beta\vec{H}\cdot\vec{S} + A\vec{S}\cdot\vec{I} + (eQV_{zz}/12)[3I_z^2 - I(I+1) + \eta(I_x^2 - I_y^2)] - g_n\beta_n\vec{H}\cdot\vec{I} \quad (7)$$

where Q is the quadrupole moment of ^{57}Fe , V_{zz} is the field gradient in the z direction, β and β_n are the Bohr and nuclear magnetons, g and g_n are the electronic and nuclear g factors, A is the hyperfine coupling constant, and η is a measure of the distortion from axial symmetry of the electric charge cloud about the ^{57}Fe nucleus. The solid lines in Figure 6 are theoretical simulations using the spin Hamiltonian parameters $D = 0.8 \text{ cm}^{-1}$, $E/D = 1/3$, $A/(g_n\beta_n) = 220 \text{ kG}$, $\Delta E_Q = 0.63 \text{ mm/s}$, $\eta = 0.0$, and $\delta = 0.5 \text{ mm/s}$. The magnetic hyperfine coupling constant A of 220 kG is typical of that observed for a high-spin ferric ion octahedrally coordinated by oxygenous ligands.³²⁻³⁶ The observed small quadrupole splitting and isotropic A are typical for a $^6A_{1g}$ electronic state.

Figure 7a shows a spectrum of $n = 3$ iron dihydroxamate complex recorded at 4.2 K with a field of 500 G applied parallel to the γ radiation. The absorption peak positions are identical with that of Figure 6a, indicating that the iron environments of the $n = 3$ and the $n = 10$ complex are similar. However, the shape of spectrum 7a suggests a faster electronic relaxation rate for the $n = 3$ complex. Figure 7b shows a spectrum of an $n = 3$ Al(Fe-doped) dihydroxamate complex recorded under the same experimental conditions. Within experimental errors spectrum 7b is identical with that of an $n = 10$ complex (Figure 6a). These results demonstrate that

(30) Aasa, R.; Malmström, B. G.; Saltman, P.; Vannagard, T. *Biochim. Biophys. Acta* **1963**, *75*, 203.

(31) Münck, E.; Huynh, B. H. *NATO Adv. Study Inst. Ser. Ser. C* **1979**, *52*, 275-288.

(32) Spartalian, K.; Oosterhuis, W. T.; Window, B. "Mössbauer Effect Methodology"; Gruverman, I. J., Ed.; Plenum Press: New York, 1973; Vol. 8, p 137.

(33) Spartalian, K.; Oosterhuis, W. T.; Neilands, J. B. *J. Chem. Phys.* **1975**, *62*, 3538.

(34) Spartalian, K.; Smarra, N.; Oosterhuis, W. T. *AIP Conf. Proc.* **1974**, *No. 18*, 1326.

(35) Lang, G.; Aasa, R.; Garbett, K.; Williams, R. J. P. *J. Chem. Phys.* **1971**, *55*, 4539.

(36) Epstein, L. M.; Straub, D. K. *Inorg. Chem.* **1969**, *8*, 453.

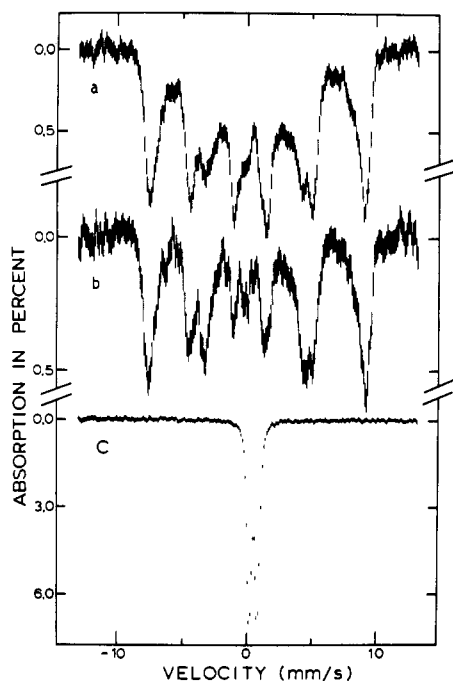


Figure 7. Mössbauer spectra of dihydroxamate complexes recorded in frozen methanol at 4.2 K with a field of 500 G applied parallel to the γ beam (Fe:L = 1:1): (a) $n = 3$ ferric dihydroxamate complex; (b) mixed FeAlL_3 dihydroxamate complex with $n = 3$; (c) $n = 5$ ferric dihydroxamate complex.

the immediate iron environment is *not* affected by the chain length, in agreement with other spectroscopic data. The observed electronic relaxation effects simply reflect a weak spin-spin interaction between the two iron sites in complexes with shorter chains.

However, a completely different situation was discovered for the $n = 5$ complex. Figure 7c shows a spectrum of the $n = 5$ iron dihydroxamate complex. A simple quadrupole doublet is observed, revealing an integral spin system. The observed quadrupole splitting, $\Delta E_Q = 0.63$ mm/s, and the isomer shift, $\delta = 0.50$ mm/s, are typical of a high-spin ferric ion. Consequently, the two ferric ions in the complex must be strongly coupled through some bridging ligands to form the integral spin system. This spectrum provides additional support for the antiferromagnetic nature of the $n = 5$ complex, which is now confirmed by X-ray crystallographic and magnetic susceptibility data.^{1,22}

Electrochemistry. The redox behavior of dimeric complexes containing two electroactive centers is characteristic of the degree of electronic interaction between the two sites. The two extreme cases are (1) that the electroactive centers are well separated and therefore completely noninteracting and (2) that there is a strong interaction between sites.³⁷

The discussion that follows assumes reversible one-electron (per site) redox behavior. For case 1, the appearance of the cyclic voltammogram (CV) depends upon the relative reduction potentials of the individual sites. When $\Delta E [E(\text{site 1}) - E(\text{site 2})]$ is greater than ~ 120 mV, two, well-separated reduction and oxidation waves are observed with individual peak-to-peak separations of 60 mV, as expected for a reversible one-electron reduction process. As the difference in reduction potentials of the two sites decreases to less than about 100 mV, the two waves begin to coalesce into a single, broadened wave, which appears to be that of an irreversible reduction process. As the difference in reduction potentials decreases to the limit where the potentials of the two sites are equal, the peak-to-peak

Table IV. Electrochemical Data for Ferric Dihydroxamate Complexes Fe_2L_3 [$\text{L} = i\text{-C}_3\text{H}_7\text{N}(\text{O})\text{C}(\text{=O})(\text{CH}_2)_n^-$ ($\text{C}(\text{=O})\text{N}(\text{O})\text{-}i\text{-C}_3\text{H}_7$)] in MeOH/ H_2O (3:1 by Volume)

n	pH* ^a	$E_{1/2}$, V	ΔE , mV	i_a/i_c
10	10.6	-0.85	60	1
8	10.5	-0.85	57	0.8
6	10.6	-0.82	62	0.6
5	10.5	-0.81	54	0.5
4	10.6	-0.80	41	0.8
3	10.6	-0.78	60	0.7

^a The pH measurements were made with a glass combination electrode that was standardized with aqueous buffer solutions (pH 7.0, 4.01); hence, pH* is not a valid thermodynamic quantity.

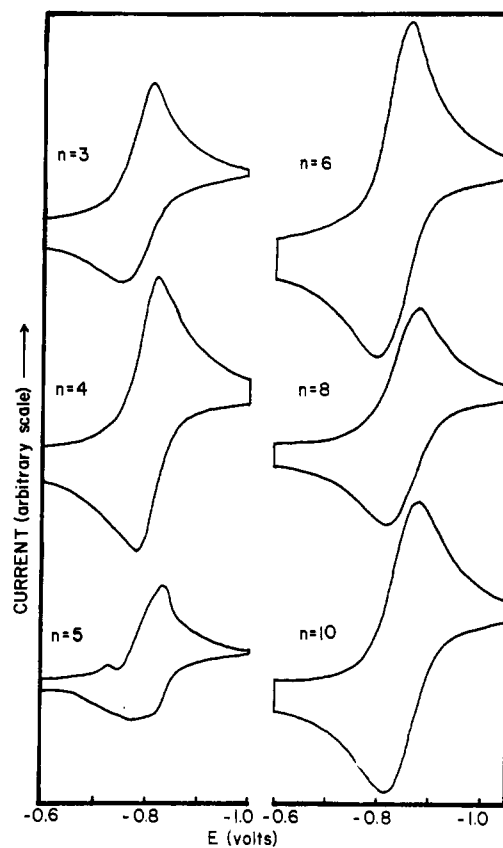


Figure 8. Cyclic voltammograms for ferric dihydroxamate complexes in methanol ($[\text{Fe}^{3+}] = 0.72$ mM; $[\text{L}] = 10$ mM; 0.1 M Et_4NBF_4 ; 75% MeOH/ H_2O ; E vs. SCE).

separation decreases and approaches 60 mV. Such behavior is characteristic of a reversible *one-electron* reduction process, although it should be remembered that in this case there are *two* one-electron reductions occurring simultaneously at the same potential.³⁷ For case 2, the two waves may be separated, or if the addition of the first electron produces a species that accepts a second electron more readily (i.e., at a more positive potential) than the original (fully oxidized) reactant, the CV is characteristic of a two-electron reduction (peak-to-peak separation of 30 mV). Polcyn and Shain have treated each of these cases theoretically.³⁸

The redox chemistry of dihydroxamate complexes of iron has been examined by using cyclic voltammetry and compared to that of ferric rhodotorulate. The redox behavior as a function of chain length will be discussed in terms of the general theory described above. Quasi-reversible pH-dependent CV waves were observed for the ferric complexes of aliphatic dihydroxamate ligands in the presence of excess ligand. The half-wave potential shifts to more positive values

(37) Flanagan, J. B.; Margel, S.; Bard, A. J.; Anson, F. C. *J. Am. Chem. Soc.* **1978**, *100*, 4248.

(38) Polcyn, D. S.; Shain, I. *Anal. Chem.* **1966**, *38*, 370.

with decreasing pH due to protonation of the Fe(II) species. Table IV summarizes the results of the electrochemical measurements under similar conditions that give quasi-reversible behavior: $[Fe^{3+}] = 0.72$ mM; $[L] = 10$ mM; solvent = 75% MeOH/H₂O (v/v); 0.1 M Et₄NBF₄. The cyclic voltammograms are shown in Figure 8. A trend toward a more negative reduction potential is observed as n , the chain length, increases. For this two-electron process $E_{1/2}$ gives the ratio of formation constants for the ferric and ferrous species:

$$E_{1/2}(\text{complex}) - E_{1/2}(\text{solvate}) = -\frac{59}{2} \log (K_{ox}/K_{red}) \\ = -\frac{59}{2} \log [\beta_{230}^{Fe(III)}/\beta_{230}^{Fe(II)}] \quad (8)$$

It was found that β_{230} for the ferric complexes is constant for the entire range of chain lengths; hence, it appears that it is the stability of the ferrous complexes that decreases as n increases.

Of interest is the sharp decrease in ΔE from approximately 60 to 41 mV as n drops to 4. The CV waves for the first three members of the series ($n = 6-10$) are characteristic of quasi-reversible one-electron reductions. The irreversibility increases as n decreases to 6, with i_a/i_c decreasing to 0.6 but maintaining a peak-to-peak separation of approximately 60 mV. For $n = 4$, an increase in i_a/i_c is observed as well as a decrease in ΔE to 41 mV. It thus appears that for $n = 6-10$ the iron atoms are reduced independently of each other at identical or very similar potentials. For $n = 3$ the process is either similar to the $n = 6 \rightarrow 10$ complexes or a very irreversible two-electron process. The $n = 4$ complex appears to exhibit electrochemistry characteristic of a quasi-reversible two-electron process, causing $\Delta E < 60$ mV. Any irreversibilities would be expected to broaden the wave and hence increase ΔE . Molecular models, as well as the spectroscopic properties of these complexes, indicate that the coordination environment about the ferric ions in the dimers Fe₂L₃ does not vary significantly with chain length. And yet a two-electron process implies that the reduction potential for the second electron is more positive than that of the first. This is unexpected since the first reduction forms an anionic species and reduction of the second Fe(III) might be expected to be more difficult on the basis of electrostatic consideration. Whether this difference is due to a static or dynamic structural change of the dimer and the iron-iron separation remains unclear.

The CV of the $n = 5$ complex (Figure 8) reveals the presence of two reduction waves—indicating that there is more than one electroactive species in solution. The visible spectrum (λ_{max} 422 nm) of the solution indicates that the major component is the dimeric tris(hydroxamate) complex. The second

component we ascribe to the ⁻OMe-bridged dimer observed in methanol solution in the absence of an excess of dihydroxamate ligand (λ_{max} 414 nm).^{1,22}

The CV's of Fe₂L₃ ($n = 8$) and Fe₂RA₃ were obtained in 50% MeOH/H₂O, 0.1 M in Et₄NClO₄ at pH ~10. $E_{1/2} = -0.70$ V and $\Delta E = 65$ mV for Fe₂RA₃, and $E_{1/2} = -0.81$ V and $\Delta E = 64$ mV for Fe₂L₃, indicating that the $n = 8$ synthetic analogue complex is more difficult to reduce than Fe₂RA₃. Since the formation constants of the tris(hydroxamate) complexes of Fe(III) are equal, this again suggests that the reduced form of the synthetic dihydroxamate complexes is less stable than the reduced form of Fe₂RA₃.

Summary

A series of dihydroxamic acids derived from the simple linear alkane dicarboxylic acids have been prepared. These compounds are analogues of the dihydroxamate siderophore rhodotorulic acid. These ligands all form dimeric complexes with the ferric ion of composition Fe₂L₃ in which the separation between the octahedrally coordinated Fe(III) ions increases with the chain length of the ligand. For $n = 8$ or 10 methylene groups separating the hydroxamate units, there is no magnetic or electrochemical interaction between the Fe(III) centers. As this distance is shortened, a through-space magnetic coupling is seen from Mössbauer and EPR spectroscopies. This assignment of the interaction is confirmed by experiments in which Fe(III) is doped into the corresponding Al(III) complexes. The general pattern of the electrochemical behavior follows this, with one unexplained discontinuity for the $n = 4$ complex. The anomalous behavior of the $n = 5$ complex in methanol is due to the formation of a completely different structure in which the iron(III) centers are coupled by methoxide bridges.

Acknowledgment. This research is supported by NIH Grant AI-11744 (Berkeley) and NSF Grants PCM-8108092 and PCM-8305995 (Emory). We thank Drs. John McCracken and Mary Kappel for experimental assistance.

Registry No. Fe(acac)₃, 14024-18-1; *N,N'*-dihydroxy-*N,N'*-diisopropylpentanediamide, 90149-53-4; *N,N'*-dihydroxy-*N,N'*-diisopropylheptanediamide, 90149-54-5; *N,N'*-dihydroxy-*N,N'*-diisopropylhexanediamide, 73586-25-1; *N,N'*-dihydroxy-*N,N'*-diisopropyloctanediamide, 73586-26-2; diferric tris(*N,N'*-dihydroxy-*N,N'*-diisopropyldodecanediamide), 90149-55-6; diferric tris(*N,N'*-dihydroxy-*N,N'*-diisopropyldecanediamide), 90149-56-7; diferric tris(*N,N'*-dihydroxy-*N,N'*-diisopropyloctanediamide), 90149-57-8; diferric tris(*N,N'*-diisopropylheptanediamide), 90149-58-9; diferric tris(*N,N'*-dihydroxy-*N,N'*-diisopropylhexanediamide), 90149-59-0; diferric tris(*N,N'*-dihydroxy-*N,N'*-diisopropylpentanediamide), 90149-60-3.